Influence of laser polarization on the laser-induced damage threshold: Comparison with photoionization theory

R. Nuter, A. Karimbana Kandy, L. Gallais, S. Grosjean, L. Lamaignère, F. Wagner, J.-Y. Natoli

Journal of Applied Physics

RESEARCH ARTICLE | JANUARY 09 2025

Influence of laser polarization on the laser-induced damage threshold: Comparison with photoionization theory

R. Nuter ; A. Karimbana Kandy; L. Gallais ; S. Grosjean; L. Lamaignère ; F. Wagner ; J.-Y. Natoli

J. Appl. Phys. 137, 025901 (2025)
https://doi.org/10.1063/5.0242463

Journal of Applied Physics ARTICLE pubs.aip.org/aip/jap

Influence of laser polarization on the laser-induced damage threshold: Comparison with photoionization theory

Cite as: J. Appl. Phys. **137**, 025901 (2025); doi: 10.1063/5.0242463
Submitted: 4 October 2024 · Accepted: 23 December 2024 ·
Published Online: 9 January 2025

R. Nuter,[1,a)] A. Karimbana Kandy,[2] L. Gallais,[2] S. Grosjean,[1] L. Lamaignère,[1] F. Wagner,[2] and J.-Y. Natoli[2]

AFFILIATIONS

[1]CEA-CESTA, F-33116 Le Barp Cedex, France
[2]Aix Marseille Univ, CNRS, Centrale Med, Institut Fresnel, Marseille, France

[a)]**Author to whom correspondence should be addressed:** rachel.nuter@cea.fr

ABSTRACT

The influence of laser polarization on the laser-induced damage threshold of fused silica is presented. Measurements were performed using femtosecond and nanosecond laser pulse durations. The impact of laser polarization on the laser damage varies with laser wavelength. While no difference in UV laser damage was observed between linear and circular polarizations, circular polarization improved the damage resistance of fused silica to infrared and visible laser radiation in comparison with linear polarization. By measuring the femtosecond laser damage of a SiO_2 thin film deposited onto a substrate, we show that the ratio between the bandgap of the sample and the photon energy causes the polarization dependent laser damage to change. These experimental findings are explained by considering the photoionization theory for solids.

I. INTRODUCTION

Various laser-plasma interaction studies require ultra intense circularly polarized laser pulses. Macchi *et al.*[1] proposed to increase the efficiency of the laser-accelerated ions mechanism by using a circularly polarized laser beam.[2] Similarly, Bashmakov *et al.*[3] showed that a circularly polarized laser pulse should improve electron–positron pair production in the quantum electrodynamical cascade. The next generation of laser facilities should certainly offer a high-power laser beam with a circular polarization such as that on the 10 PetaWatt Vulcan laser beam.[4] Thus, investigating how a circularly polarized laser pulse will modify the damage resistance of the optical components to laser radiation appears crucial for future laser facility development.

Some research groups have already explored this question. Liu *et al.*[5] showed that for ultra-short laser pulses (120 fs), the numerical aperture (NA) of the focusing objective, used to focus the laser beam on the surface of the silica glass, causes the polarization dependent laser damage to change. The damage threshold for circular polarization is higher than for linear polarization when NA is higher than 0.4. The reverse effect is observed when NA is shorter than 0.4. For collimated laser beams, Soileau *et al.*[6] and Bonod *et al.*[7] showed that linear-to-circular polarization conversion mitigates the laser-induced filamentation inside the glass. They linked this filamentation mitigation to the polarization-dependent Kerr effect[6] driven by the nonlinear refractive index (n_2). However, fused silica filamentation develops from two concomitant processes: Kerr effect-induced beam self-focusing and laser-induced ionization.[8] The dependence of the Kerr effect on laser polarization is now well-characterized in isotropic media, for example, in glass. The associated nonlinear index of refraction is reduced in circular polarization by a factor of 3/2 compared to linear polarization.[9,10] However, few studies have been devoted to the laser polarization dependence of solid ionization, and more largely to the laser polarization dependence of the laser-induced damage threshold (LIDT) by disregarding the effect of laser nonlinear propagation. Zhang *et al.*[11] experimentally observed that the LIDT fluence of a Ta_2O_5/SiO_2 film is increased from 1.68 J/cm^2 for linear polarization (LP)

up to 1.70 J/cm^2 for circular polarization (CP), when irradiated with an 800 nm, 50 fs laser beam. They correlated the increase in LIDT with the decrease in photoionization rate induced by circular polarization, as measured by Temnov *et al.* in Ref. 12. On the other hand, Venable and Kay[13] experimentally measured that in a four-photon process, the photoionization of quartz is more efficient with a circularly polarized laser beam than with a linear one. By measuring the refractive index change in waveguides, Little *et al.*[14,15] inferred that the photoionization rate for fused silica[14] and Yb:QX phosphate glass[15] is increased with the circular polarization, while, for BK7 glass,[15] no difference between linear and circular polarization is observed. Kozák *et al.*[16] showed theoretically and experimentally that linear polarization produces a larger carrier density in diamond than circular polarization. These clearly contrasting observations highlight the need to characterize the impact of laser polarization on laser damage, by disregarding any propagative effects, for example, the nonlinear propagation of the laser beam into the optical component.

The current work displays laser damage measurements on the front surface of a fused silica glass, irradiated by a laser beam with a circular and linear polarization and that operates in the infrared (IR), visible, and ultraviolet (UV) radiation spectrum. First, the damage probabilities measured with a femtosecond laser beam reveal the influence of laser polarization on LIDT values for three different wavelengths. Femtosecond laser damage originates from material intrinsic properties.[17] A theoretical explanation for these polarization-influenced measurements is provided by the photoionization rates computed from the theory developed in Refs. 18 and 19. Indeed, femtosecond laser damage is known to be driven by the photoionization process.[20] Because theoretical photoionization rate values vary with the material bandgap, experimental femtosecond LIDT is also investigated by substituting fused silica glass for a sample with a lower bandgap, that is, an SiO_2 thin film deposited on a BK7 glass. Then, in the second part, we investigate the influence of polarization on LIDT in the nanosecond regime. Because, our laser focal spots are small (near 10 μm), we assume that ns-LIDT is driven by material intrinsic properties. Ns-LIDT is measured by using different wavelengths, and we compare these measurements to the photoionization theory for solid although a direct comparison between nanosecond laser damage and ionization rate is not obvious as it involves additional physical processes, for example, heat transfer from electrons to the lattice or collisional ionization. Thus, in this work, the impact of laser polarization on laser damage is studied in the fast and ultrafast regimes.

II. THEORETICAL TOOLS

Sudrie *et al.*[20] proposed a theoretical understanding of damage induced in the bulk of fused silica by interaction with femtosecond infrared laser pulses. The first step in the laser damage process is the free electron generation through the laser–solid interaction. The equation, governing the temporal evolution of the free electron density, ρ, is

$$\frac{\partial \rho}{\partial t} = W_{PI}(|\mathcal{E}|) + \frac{\sigma}{B_g}\rho|\mathcal{E}|^2 - \frac{\rho}{\tau_R}, \tag{1}$$

where $W_{PI}(|\mathcal{E}|)$ is the photoionization rate, σ is the collisional ionization cross section, B_g is the bandgap of the solid, τ_R is the recombination time, and $\mathcal{E}$ is the normalized laser electric field such that the laser intensity is $I = |\mathcal{E}|^2$. Equation (1) shows that the photoionization process (first term on the right hand side), promoting electrons from the valence band to the conduction band of the solid, triggers the free electron generation, which could result in the bulk laser damage.

In Ref. 19, we have developed a theory modeling the ionization of a solid irradiated with a linearly and a circularly polarized laser beam. It provides an analytical expression for the $W_{PI}(|\mathcal{E}|)$ term, resulting in a laser polarization depending rate. For a linear laser polarization, the photoionization rate is given by

$$\begin{aligned} W_{PI}^{\text{lin}} &= \frac{1}{16\sqrt{2}\pi}\frac{1}{\gamma^2}\frac{\mu_r^{\frac{3}{2}}\omega^4\sqrt{B_g}}{(\hbar\omega)^2}\int_0^\pi \sin\theta d\theta \\ &\times \sum_{l\geq l_0}\sqrt{\frac{l\hbar\omega}{B_g} - 1 - \frac{1}{4\gamma^2}}\left[\overline{J_{l-1}}(\alpha,\beta) - \overline{J_{l+1}}(\alpha,\beta)\right]^2, \\ \alpha &= -\frac{\sqrt{2}}{\gamma}\frac{B_g}{\hbar\omega}\sqrt{\frac{l\hbar\omega}{B_g} - 1 - \frac{1}{4\gamma^2}}\cos\theta, \\ \beta &= -\frac{1}{8\gamma^2}\frac{B_g}{\hbar\omega}, \\ l_0 &= l_0^{\text{lin}} = \min_l\left(\frac{l\hbar\omega}{B_g} - 1 - \frac{1}{4\gamma^2} > 0\right), \end{aligned} \tag{2}$$

where $\gamma = \frac{\omega\sqrt{\mu_r B_g}}{eE_0}$, with μ_r being the reduced electron–hole mass, e the electron charge, ω the photon angular frequency, and E_0 the laser electric field amplitude such that $|\mathcal{E}|^2 = \frac{1}{2}\epsilon_0 c n_0 |E_0|^2$ with c being the light velocity in vacuum, n_0 the linear refractive index, and ϵ_0 the permittivity in vacuum. $\overline{J_n}(u, v)$ are the generalized Bessel functions.[21] l_0 is the minimum number of photons required to promote electron from the valence to the conduction band that is energetically shifted by the ponderomotive energy equal to $\frac{B_g}{4\gamma^2}$. For a circular laser polarization, the photoionization rate formula is different,

$$\begin{aligned} W_{\text{cir}} &= \frac{1}{8\sqrt{2}\pi}\frac{1}{\gamma^2}\frac{\mu_r^{\frac{3}{2}}\omega^4\sqrt{B_g}}{(\hbar\omega)^2}\int_0^\pi \sin\theta d\theta \\ &\times \sum_{l\geq l_0}\sqrt{\frac{l\hbar\omega}{B_g} - 1 - \frac{1}{2\gamma^2}}\left[J_{l-1}^2(\eta) + J_{l+1}^2(\eta)\right], \\ \eta &= -\frac{\sqrt{2}}{\gamma}\frac{B_g}{\hbar\omega}\sqrt{\frac{l\hbar\omega}{B_g} - 1 - \frac{1}{2\gamma^2}}\sin\theta, \\ l_0 &= l_0^{\text{cir}} = \min_l\left(\frac{l\hbar\omega}{B_g} - 1 - \frac{1}{2\gamma^2} > 0\right), \end{aligned} \tag{3}$$

where $J_l(x)$ denotes the Bessel functions of the first kind.[22] In this case, the ponderomotive energy is larger than in the linear case, it is

equal to $\frac{B_g}{2\gamma^2}$. We have shown in Ref. 19 that the dependence of the solid photoionization rate with the laser polarization varies with the laser wavelength. This double dependency (polarization and wavelength) originates from the difference in the selection rule for the dipole quantum magnetic number: $\Delta m = 0$ for linear polarization and $\Delta m = +1$ ($\Delta m = -1$) for left (right) circular polarization. This selection rule reduces the number of allowed electronic transition channels for circular polarization in comparison with linear polarization, leading to a lower transition probability. Thus, an increase in the $B_g/(\hbar\omega)$ ratio results in a larger prevalence of the LP-ionization rate over CP-ionization rate. The present work aims to make a connection between the LIDT and the photoionization process, key process in the laser damage. For this reason, we compare the laser damage threshold with the electron density is only generated by the photoionization process. We thus solve

$$\frac{\partial \rho}{\partial t} = W_{PI}(|\mathcal{E}(t)|), \tag{4}$$

where $\mathcal{E}(t)$ models an electric field with a Gaussian and a "gate" temporal function for femtosecond and nanosecond studies, respectively. We assume that avalanche ionization does not depend on laser polarization.[23]

III. FEMTOSECOND RESULTS

First, we consider a 500 fs, 1030 nm laser beam to investigate the LIDT of the fused silica glass and the SiO_2 thin film deposited onto a substrate. By employing appropriate nonlinear crystals, the IR laser beam is frequency converted to a second (515 nm) and a third (343 nm) order harmonic beam. All experiments discussed in this work have been performed using single-shot laser irradiation (1-on-1).[24] The experimental setup is presented in the Appendix.

A. Fused silica glass

We first measured the laser damage probability of a fused silica glass irradiated on its front surface with a 1030 nm laser beam. The irradiated samples were bare fused silica windows (HERAEUS S312 10 mm thickness), superpolished by Thales-SESO. The LIDT measurements are summarized in Fig. 1 for circular (red circles) and linear (black crosses) laser polarization according to laser intensity (bottom axis) and the laser fluence (top axis). By considering a laser fluence uncertainty of 9%,[25] the laser intensity uncertainty was estimated at 19%. Linear polarization displayed a weaker LIDT than circular polarization. For a quantitative LIDT comparison, we defined the LIDT intensity as the averaged value of the laser intensities for which the damage probability varies from 0 to 1. The LIDT intensity uncertainty was computed as the half difference between these two intensity values. It is equal to 10.67 ± 0.23 TW/cm^2 for linear polarization (LP) and 11.85 ± 0.41 TW/cm^2 for circular one, meaning a LIDT increase of 11% for the circular case. It is important to remember that the laser beams are focused on the sample's front surface, such that this LIDT difference between linearly and circularly polarized laser beams could not be attributed to the Kerr effect and its associated

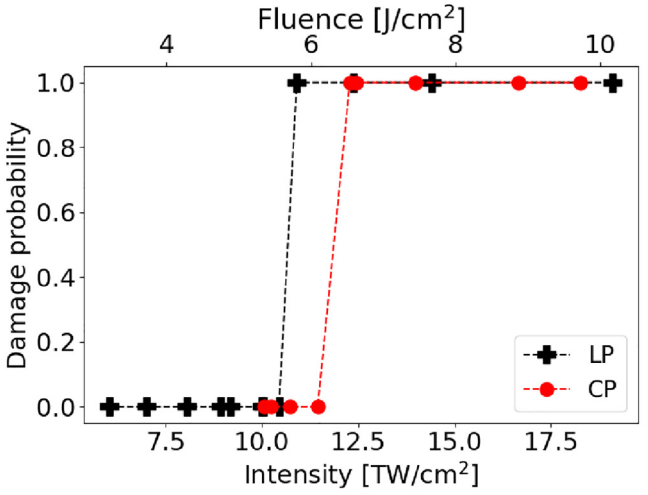

FIG. 1. Damage probability of a fused silica sample vs laser intensity (bottom axis) and laser fluence (top axis) for a linearly (black crosses and black dashed curve) and circularly (red circles and red dashed curve) polarized laser beam. $\lambda_0 = 1030$ nm and pulse duration equal to 500 fs.

nonlinear refractive index (n_2), but only to the ionization of the fused silica glass.

We duplicated these measurements for two other laser wavelengths: 515 and 343 nm. The LIDT intensity values are summarized in Table I. Because the LIDT intensities were measured on the same laser beam, we do not include the measurements of laser intensity uncertainty but only the computation uncertainty which is equal to the half difference between the laser intensities for which the damage probability varies from 0 to 1.

First, we note that the LIDT intensity values are positively correlated to laser wavelength, which is in agreement with the results in Ref. 26. For the three laser wavelengths, a circularly polarized laser beam provides a higher LIDT intensity value than a linear one. An increase of 11%, 20%, and 7% is observed for 1030, 515, and 343 nm laser wavelength, respectively.

Figure 2(a) plots the fused silica ionization rate, computed from Eqs. (2) and (3), according to laser intensity for three laser wavelengths (343, 515, and 1030 nm) and for both laser polarizations (linear and circular). We consider a bandgap equal to 9 eV,[20] and the electron–hole reduced mass equal to $\mu_r = 0.3\, m_e$.[18] The vertical dashed curves in Fig. 2(a) indicate the LIDT intensity values measured for linear polarization (Table I). For the two

TABLE I. LIDT intensity values for fused silica (in TW/cm^2) vs laser polarization and laser wavelength. The LIDT intensity uncertainty is equal to the half difference between the laser intensities for which the damage probability varies from 0 to 1.

	1030 nm	515 nm	343 nm
Linear polarization	10.67 ± 0.23	3.38 ± 0.16	2.35 ± 0.01
Circular polarization	11.85 ± 0.42	4.07 ± 0.31	2.51 ± 0.01

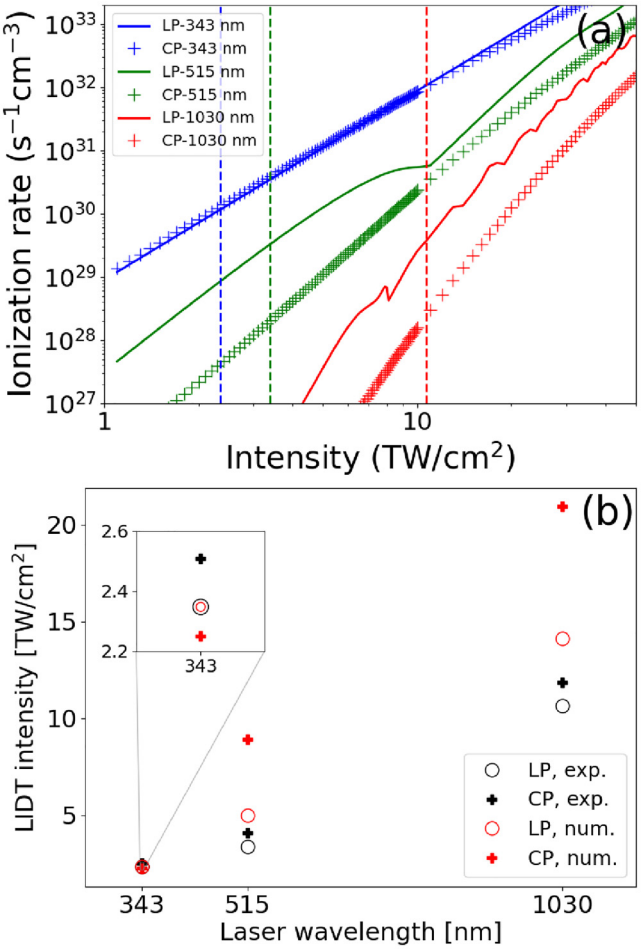

FIG. 2. (a) Theoretical values [Eqs. (2) and (3)] of the fused silica ionization rate with $B_g = 9$ eV[20] and $\mu_r = 0.3\,m_e$ for three laser wavelengths: 1030 nm (red), 515 nm (green), and 343 nm (blue) and for linear (solid curve) and circular (crosses) laser polarization. Vertical dashed curves display the LIDT intensity values for linear polarization (Table I). (b) Numerical (red) and experimental (black) LIDT intensity values according to laser wavelength for linear (circle) and circular (cross) polarization.

longer laser wavelengths ($\lambda_0 = 1030$ and 515 nm), the linearly polarized laser beam generated a higher free electron density than the circular one, while no difference was observed between both polarizations for $\lambda_0 = 343$ nm.

These ionization rates were used to compute numerical values for LIDT intensity, shown with red symbols in Fig. 2(b). The numerical LIDT intensity corresponds to the laser intensity for which the temporal integration of Eq. (4) results in $\rho_{\text{ref}} = 3.57 \times 10^{17}$ cm^{-3}. This reference value of electron density, used to link experimental and numerical LIDT values, was computed by solving Eq. (4) for a 343 nm, linearly polarized laser beam with a laser intensity equal to 2.35 TW/cm^2 (see Table I). Figure 2(b) shows a similar trend between numerical and experimental LIDT intensities. First, LIDT intensity increases as the laser wavelength increases, irrespective of polarization. This feature characterizes the multiphoton ionization regime and originates from the need for a larger number of photons to promote the electron from the valence to the conduction band. Therefore, to achieve the same level of ionization, laser intensity should be higher for longer wavelengths. Then, while the UV wavelength (343 nm) shows no difference in LIDT intensity value between linear and circular polarizations, the visible and IR wavelengths display a higher LIDT for circular polarization than for linear polarization. As for the experimental measurements, numerical LIDT values show a larger LIDT increase for circular polarization for the visible wavelength (numerical = 78.7%, experimental = 20%) than for the IR wavelength (numerical = 48.6%, experimental = 11%). Note that numerical LIDT values overestimate the experimental values because the collisional ionization process is not included in the electron density computation.

B. SiO_2 thin film

In order to investigate the link between femtosecond LIDT measurements and the photoionization theory, similar measurements were also performed on a sample with a lower bandgap than fused silica glass, that is, an SiO_2 thin film deposited onto a substrate. The silica (SiO_2) layer was deposited by electron beam evaporation with ion assistance deposition onto a BK7 substrate. The layer thickness was 149.9 nm, with a refractive index of 1.930 at 1053 nm determined by ellipsometry. The bandgap, $B_g = 7.5$ eV,[27] is weaker than for fused silica glass.

The LIDT-intensity values are summarized in Table II. A positive correlation between LIDT values and wavelength, similar to the case of fused silica glass, was observed. By comparing the LIDT values in Table II with those measured for the fused silica glass in Table I, we observe that a lower bandgap value results in a reduction in LIDT intensity value. Moreover, we note that only the IR wavelength (1030 nm) displayed a noticeable difference in LIDT values, nearly 6%, between linear and circular polarization. In the case of 515 and 343 nm wavelengths, circular polarization increased the LIDT intensity value by 2% and 1.5%, respectively, which reveals an insignificant difference between both polarizations.

This trend was highlighted in the SiO_2 photoionization rate plotted in Fig. 3(a) and for which we consider $B_g = 7.5$ eV and $\mu_r = 0.3m_e$. The two shortest laser wavelengths (343 and 515 nm) displayed comparable ionization rates for linear and circular polarization. Only the IR wavelength showed higher ionization rates for linear polarization than for circular polarization. As in the previous case, Fig. 3(b) compares the experimental and numerical LIDT

TABLE II. Intensity values in TW/cm^2 for the laser-induced damage threshold (LIDT) in an SiO_2 thin film deposited on glass. The LIDT intensity uncertainty is equal to half difference between the laser intensities for which the damage probability varies from 0 to 1.

	1030 nm	515 nm	343 nm
Linear polarization	7.55 ± 0.11	1.73 ± 0.02	1.54 ± 0.01
Circular polarization	8.01 ± 0.00	1.76 ± 0.03	1.56 ± 0.01

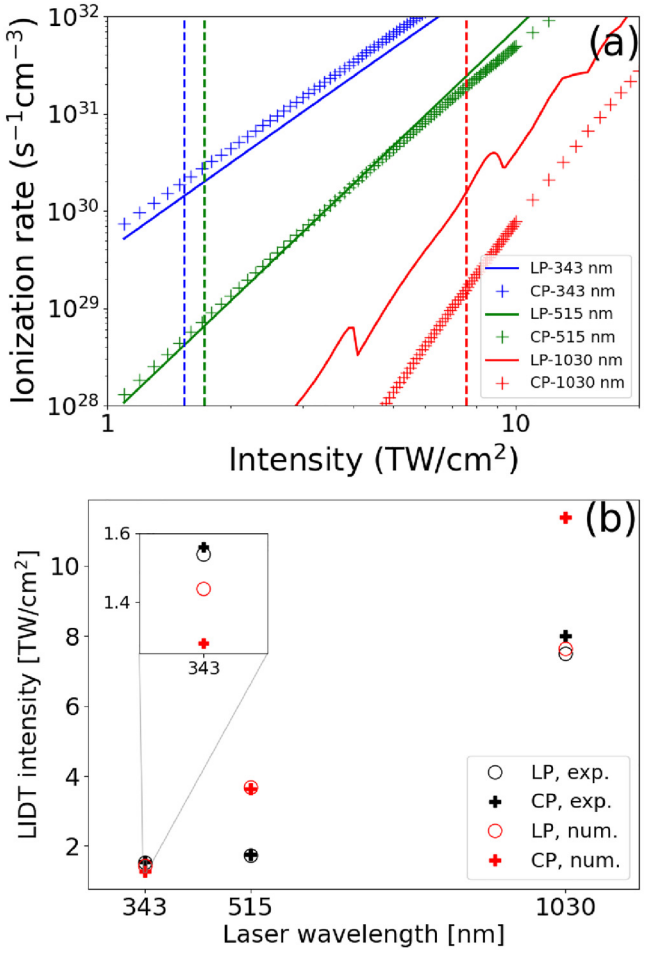

FIG. 3. Theoretical values for SiO_2 thin film ionization rate with $B_g = 7.5$ eV and $\mu_r = 0.3m_e$ for three laser wavelengths: 1030 nm (red), 515 nm (green), and 343 nm (blue) and for linear (solid curve) and circular (crosses) laser polarization. Vertical dashed curves represent the LIDT intensity values for linear polarization (Table II). (b) Numerical (red) and experimental (black) LIDT intensity values according to laser wavelength for linear (circle) and circular (cross) polarization.

intensity values for three wavelengths and for two laser polarizations, showing a relatively good agreement between theory and experiment. Note that numerical LIDT intensity values correspond to an electron density equal to $\rho_{ref} = 3.57 \times 10^{17}$ cm^{-3}, the same reference value as the one considered for fused silica.

The femtosecond LIDT measurements supported by the theoretical ionization rates confirm that the LIDT intensity values are linked to the photoionization process, as was presented by Sudrie *et al.* in Ref. 20. Circular polarization could be a convenient tool to mitigate the laser-induced damage to the optical components in the range of laser intensities and laser wavelengths, which reduces the photoionization rate in comparison with linear polarization.

IV. NANOSECOND RESULTS

Nanosecond LIDT measurements were performed with a Q-switched Nd:YAG single mode laser, lasing at 1064 nm. Appropriate frequency conversion units were used to generate harmonic beams. The LIDT measurements were only performed on the front surface of the fused silica (see the Appendix). For this case, we did not consider the SiO_2 film deposited on a substrate. The same type of fused silica glass as that used for femtosecond measurements was utilized. LIDT measurements were performed using 1064, 532, and 355 nm wavelengths with pulse durations of approximately 32, 11, and 10 ns, respectively. All measurements correspond to a single-shot irradiation per site. We have performed 20 shots per laser beam fluence.

Figure 4 presents the laser damage probability on a fused silica sample measured for a 31.5 ns, 1064 nm laser for which polarization is linear (black crosses) or circular (red circles). The damage probability is equal to the ratio between the number of laser damaged sites and the number of laser irradiated sites (equal to 20). The error bars show the standard deviation in the experimental measurements. For a linearly polarized laser beam (black crosses), the damage probability is less than 10% (gray dotted line) for laser intensity below 33 GW/cm^2, increasing linearly for higher intensity values until the damage probability is 100%. Since the nanosecond LIDT measurements present large error bars, it is difficult to pinpoint the LIDT value. We, thus, define the 50% LIDT that is the laser intensity for which the damage probability is equal to 50% (gray dashed line). By applying a linear regression on the increasing damage probability data, we find a 50% LIDT equal to 53.7 GW/cm^2 in the case of linear polarization. Red circles, denoting circular polarization data, show damage probabilities shifted to higher laser intensity compared to the linear case.

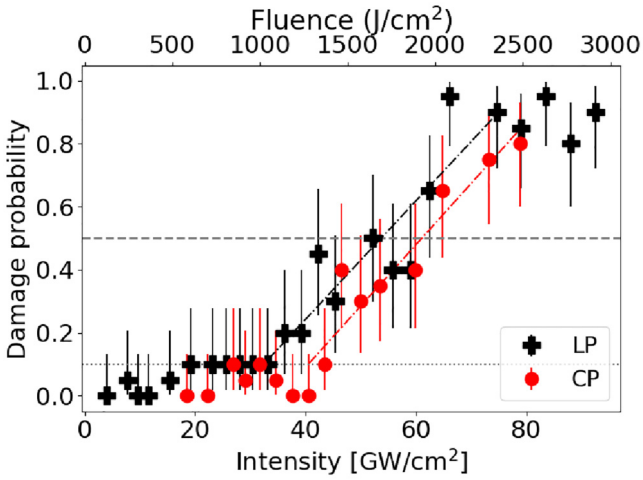

FIG. 4. Damage probability of a fused silica sample vs laser intensity (bottom axis) and laser fluence (top axis) for a linearly (black crosses) and circularly (red circles) polarized laser beam. $\lambda_0 = 1064$ nm and pulse duration equal to 31.5 ns. The black and red dash-dotted curves display the linear regression of experimental measurements for linearly and circularly polarized laser beams, respectively. The gray dashed and dotted curves display the 50% and 10% damage probabilities, respectively.

The damage probability is less than 10% up to an intensity equal to 43.3 GW/cm^2, before following an increasing slope like that of linear polarization. For the circularly polarized beam, the linear regression gives a 50% LIDT intensity equal to 61.1 GW/cm^2, corresponding to an increase of nearly 14%.

Similar LIDT measurements for a 11.3 ns long, 532 nm laser wavelength are plotted in Fig. 5. The damage probability is lower than 10% (gray dotted line) up to laser intensities of 13.4 and 20.7 GW/cm^2 in the case of linear and circular polarization, respectively. The circularly polarized laser beam still presents a larger LIDT value than the linearly polarized one. By applying linear regression to the increasing damage probability values, we find that 50% LIDT (gray dashed line) is reached for an intensity of 37.8 GW/cm^2 for the linear case and of 56.1 GW/cm^2 for the circular case, corresponding to an increase of 48%.

The damage probabilities measured in the UV domain ($\lambda_0 = 355$ nm) are summarized in Fig. 6. By contrast with the two previous cases, a very weak difference (5%) is observed between both laser polarizations.

Table III summarizes the laser intensity for which the damage probability is equal to 50% for three laser wavelengths and for both laser polarizations. The laser intensity uncertainty is computed from the numerical error estimated on the linear regression. The R^2 value measures the strength of the relationship between our experimental data and the dependent variable on a convenient 0 to 1 scale. Since the laser pulse length is in the nanosecond temporal range, the LIDT intensity values (GW/cm^2) are much weaker than the fs LIDT values (TW/cm^2). Table III shows a similar trend to Table I values: LIDT-intensity values decrease as laser wavelength decreases for both laser polarizations.[28] We note that for UV wavelength, LIDT intensity values are similar for linear and circular polarizations, whereas for visible radiation, linear polarization is characterized by a weaker 50% LIDT intensity than circular polarization. Because of large uncertainties on LIDT values measured for λ =1064 nm, we cannot conclude.

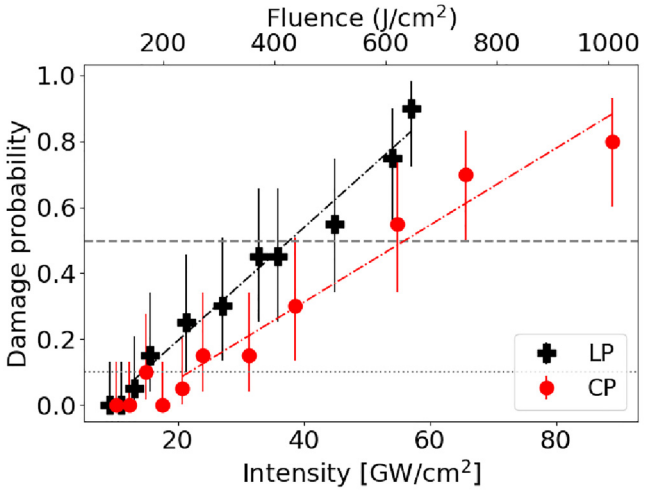

FIG. 5. Same as Fig. 4 but for $\lambda_0 = 532$ nm and pulse duration equal to 11.3 ns.

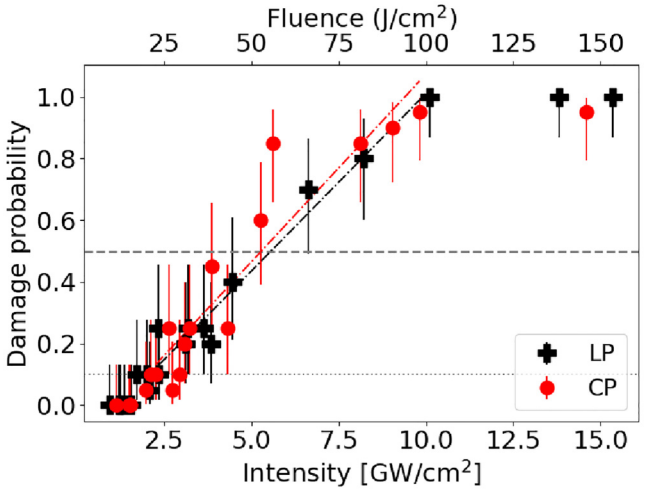

FIG. 6. Same as Fig. 4 but for $\lambda_0 = 355$ nm and pulse duration equal to 10 ns.

Similar to the femtosecond laser damage measurements, we compare nanosecond LIDT-intensity values to the fused silica photoionization rates computed in Fig. 7(a). For a constant laser intensity, the higher laser wavelengths result in a lower ionization rate, originating from the necessity to have a higher number of photons to promote electrons from the valence to the conduction band. Thus, higher wavelengths require higher intensities to reach similar ionization levels, as observed in Table III. Figure 7(b) compares the experimental and numerical 50% LIDT intensities, where the numerical values are obtained with a reference electron density equal to 8.6×10^{13} cm^{-3} ($\lambda = 355$ nm and linear polarization). It displays a similar behavior as in the case of femtosecond measurements (Table III): a domination of the linear polarization over circular polarization in the photoionization processes for the two longer laser wavelengths ($\lambda_0 = 1064$ and 532 nm), and no difference in the photoionization process for the UV wavelength. We still observe a higher LIDT increase for circular polarization for the visible wavelength (numerical increase 220%, experimental increase 48.4%) than for the IR wavelength (numerical increase 121%, experimental increase 14%). Note that LIDT values in Fig. 7(b) are in log scale because numerical results strongly overestimate the

TABLE III. Laser intensity value in GW/cm^2 for a 50% damage probability in fused silica bulk vs laser wavelength and laser polarization. R^2 is the coefficient of confidence in the linear regression.

	1064 nm	532 nm	355 nm
Linear polarization	53.69 ± 8.3	37.78 ± 6.08	5.56 ± 0.32
R^2 value	0.82	0.97	0.96
Circular polarization	61.07 ± 7.59	56.10 ± 13.67	5.29 ± 0.86
R^2 value	0.9	0.95	0.86

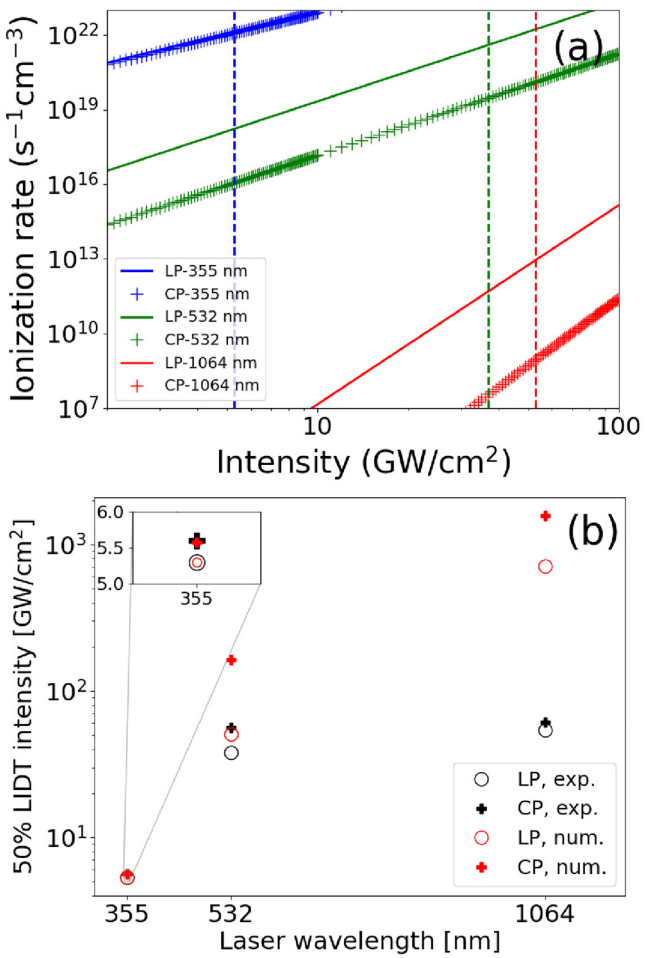

FIG. 7. Photoionization rate values vs laser intensity for the fused silica bulk with $B_g = 9$ eV and $\mu_r = 0.3m_e$ for three laser wavelengths: 1064 nm (red), 532 nm (green), and 355 nm (blue) and for linear (solid curve) and circular (crosses) laser polarization. Vertical dashed curves display LIDT intensity values for linear polarization (Table III). (b) Numerical (red) and experimental (black) 50% LIDT intensity values according to laser wavelength for linear (circle) and circular (cross) polarization.

experimental ones. This clearly highlights that additional processes play an important role in the nanosecond laser damage.

Thus, even though additional physical processes such as collisional ionization, thermal conductivity, and mechanical dynamics play an important role in the nanosecond laser damage process, we find a similar trend between the polarization dependent LIDT intensity values and the polarization dependent photoionization rates[19] for visible and UV radiations.

V. CONCLUSION

We investigated the impact of laser polarization on the LIDT of optical components by varying the pulse duration, pulse wavelength, and material bandgap. We measured the damage probability by focusing the laser beam on the front surface of the optical component. This experimental configuration enabled us to disregard the effect of laser beam propagation on the LIDT and to focus our attention exclusively on the impact of laser-induced plasma generation.

For both femtosecond and nanosecond pulse duration regimes, we found that the laser-induced damage threshold could be linked to the photoionization rate. By varying the laser pulse length, we explored the photoionization process in two different laser intensity domains (GW/cm^2 and TW/cm^2). For the fused silica sample, these intensity domains correspond to the multiphoton ionization regime. In a high-order multiphoton-dominated ionization regime, where a large number of photons is required to promote electrons from the valence to the conduction band, linear laser polarization produces a higher free carrier density than circular laser polarization for the same laser energy. This feature results in a higher LIDT for circular than for linear polarization. In an ionization regime where few photons ionize the material, such as an ultraviolet laser beam for fused silica glass, linear and circular laser polarizations provide a similar ionization level, resulting in comparable LIDT intensity values.

We compared the LIDT values measured for fused silica glass (bandgap equal to 9 eV) and for a SiO_2 thin film deposited on a glass (bandgap equal to 7.5 eV). We observed that a lower bandgap value leads to a lower LIDT value, resulting in a reduced difference between linear and circular polarization-induced laser damage. Thus, the impact of laser polarization on laser-induced damage depends strongly on the bandgap value and on the laser wavelength. This could be estimated with the photoionization theory for solid media. In summary, when high-order multiphoton ionization is dominant, circular laser polarization provides significant resistance against laser-induced damage compared to linear polarization.

AUTHOR DECLARATIONS

Conflict of Interest

The authors have no conflicts to disclose.

Author Contributions

R. Nuter: Conceptualization (equal); Formal analysis (lead); Methodology (lead); Validation (equal); Writing – original draft (lead); Writing – review & editing (equal). **A. Karimbana Kandy:** Investigation (equal); Methodology (equal); Validation (equal); Writing – review & editing (equal). **L. Gallais:** Conceptualization (equal); Supervision (equal); Validation (equal); Writing – review & editing (equal). **S. Grosjean:** Supervision (supporting); Validation (supporting); Writing – review & editing (equal). **L. Lamaignère:** Conceptualization (equal); Methodology (equal); Supervision (equal); Writing – review & editing (equal). **F. Wagner:** Investigation (equal); Methodology (equal). **J.-Y. Natoli:** Conceptualization (equal); Methodology (equal); Supervision (equal); Writing – review & editing (equal).

DATA AVAILABILITY

The data that support the findings of this study are available from the corresponding author upon reasonable request.

APPENDIX: EXPERIMENTAL SETUP

Figure 8 presents the experimental setup considered for LIDT measurements in both temporal regimes (femtosecond and nanosecond).

While the laser operates at a repetition rate of 10 kHz, an external electronic shutter picks out single pulses for the LIDT measurements. A quarter-wave plate is used to convert the laser beam polarization from linear to circular. An XY translational stage is dedicated to mounting the sample. Meanwhile, the focusing lens is mounted on an individual Z-axis translational stage that allows the precise focalization of the laser on the sample surface. It is also worth noting that all LIDT measurements discussed were performed on the front surface of the sample, which was kept at normal incidence. A half-wave plate polarizer combination accurately controls the laser pulse energy. The energy per pulse focused on the sample position is calibrated with respect to a reference glass plate, placed in the laser beam path (as shown in Fig. 8). More specifically, two power meters were simultaneously used, one for measuring the energy at the sample position and the other one for measuring the beam energy reflected from the reference glass plate. A calibration database between the two energies is created for several energy values. The input laser energy is controlled by rotating the half-wave plate. An example of such calibration data is shown in Fig. 9. Each data point results from the averaged energy of 3000 laser pulses. It is worth noting that this calibration is performed before each measurement and for each laser polarization to ensure the accuracy in estimating the fluence at the sample position.

1. Femtosecond measurement

A CCD camera imaged the live modifications induced on the sample surface. Plano–convex lenses of focal lengths (FL) 75, 75, and 100 mm were used for the measurements on SiO_2 glass using 1030, 515, and 343 nm wavelengths, respectively. The associated focal spot radii were 15, 12.7, and 10.9 μm, respectively. The same experimental parameters were used for the measurement of a SiO_2 thin film deposited on the substrate, with the exception of 515 nm, for which a 100 mm plano–convex lens was utilized. This gave a 16.5 μm focal spot radius. The uncertainty of focal spot radius measurements was estimated at 6%.[25] Linear-to-circular polarization conversion was performed using quarter-wave plates. The beam profiles at the focal spot were analyzed separately for the circular and linear polarizations. No difference in the focal spot was observed between the two polarizations.

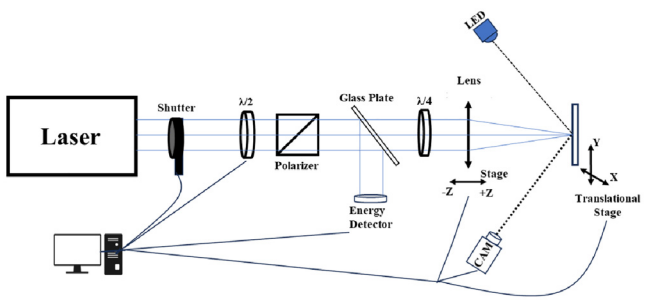

FIG. 8. Experimental setup used for LIDT measurements in both temporal regimes.

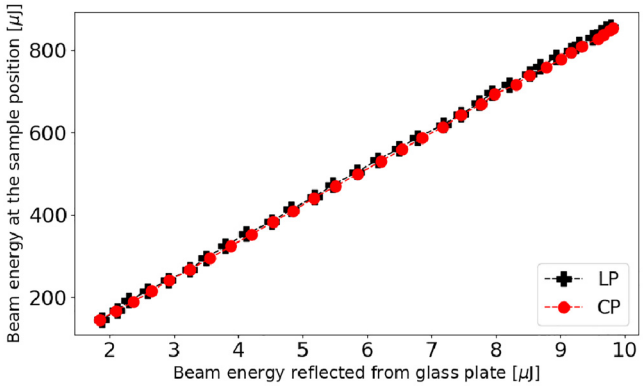

FIG. 9. Beam energy at the sample position (μJ) vs the beam energy reflected from glass plate (μJ) for linear (black cross) and circular (red circle) laser polarization.

2. Nanosecond measurements

For all laser configurations, the beam was focused on the sample surface using a plano–convex lens of focal length 100 mm. The laser spot radii obtained at the focal spot for 1064, 532, and 355 nm were 11.66 ± 0.2, 9.36 ± 0.57, and 13.81 ± 0.61 μm, respectively. The beam focal spots provide similar beam profiles for linear and circular polarizations.

REFERENCES

[1]A. Macchi, F. Cattani, T. Liseykina, and F. Cornolti, "Laser acceleration of ion bunches at the front surface of overdense plasmas," Phys. Rev. Lett. **94**, 165003 (2005).
[2]J. Badziak, "Laser-driven ion acceleration: Methods, challenges and prospects," J. Phys: Conf. Ser. **959**, 012001 (2018).
[3]V. Bashmakov, E. Nerush, I. Kostyukov, A. Fedotov, and N. Narozhny, "Effect of laser polarization on quantum electrodynamical cascading," Phys. Plasmas **21**, 013105 (2014).
[4]R. Heathcote, S. Bick, R. Clarke, and J. Green, "Modeling of a reflective waveplate for high power lasers," Proc. SPIE **9194**, 9194N (2014).
[5]D. Liu, Y. Li, M. Liu, H. Yang, and Q. Gong, "The polarization-dependance of femtosecond laser damage threshold inside fused silica," Appl. Phys. B **91**, 597 (2008).
[6]M. Soileau, W. Williams, N. Mansour, and E. V. Stryland, "Laser induced damage and the role of self-focusing," Opt. Eng. **28**, 1133 (1989).
[7]N. Bonod, P. Branceau, J. Daurios, S. Grosjean, N. Roquin, J.-F. gleyze, L. Lamaignère, and J. Néauport, "Linear-to-circular polarization conversion with

full-silica meta-optics to reduce nonlinear effects in high-energy lasers," Nat. Commun. **14**, 5383 (2023).
[8]L. Bergé, S. Skupin, R. Nuter, J. Kasparian, and J.-P. Wolf, "Ultrashort filaments of light in weakly ionized, optically transparent media," Rep. Prog. Phys. **70**, 1633 (2007).
[9]R. W. Boyd, *Nonlinear Optics* (Academic Press, 2008).
[10]M. Weber, D. Milan, and W. Smiths, "Nonlinear refractive index of glasses and crystals," Opt. Eng. **17**, 464 (1978).
[11]L. Zhang, X. Jia, Y. Wang, A. Chen, J. Shao, and C. Zheng, "Effect of femtosecond laser polarization on the damage threshold of Ta_2O_5/SiO_2 film," Appl. Sci. **12**, 1494 (2022).
[12]V. Temnov, K. Sokolowski-Tinten, P. Zhou, A. El-Khamhawy, and D. von der Linde, "Multiphoton ionization in dielectrics: Comparison of circular and linear polarization," Phys. Rev. Lett. **97**, 237403 (2006).
[13]D. Venable and R. Kay, "Polarization effects in four-photon conductivity in quartz," Appl. Phys. Lett. **27**, 48 (1975).
[14]D. Little, M. Ams, P. Dekker, G. Marshall, J. Dawes, and M. Withford, "Femtosecond laser modification of fused silica: The effect of writing polarization on Si-O ring structure," Opt. Express **16**, 20029 (2008).
[15]D. Little, M. Ams, and M. Withford, "Influence of bandgap and polarization on photo-ionization: Guidelines for ultrafast laser inscription," Opt. Mater. Express **1**, 670 (2011).
[16]M. Kozák, T. Otobe, M. Zukerstein, F. Trojánek, and P. Malý, "Anisotropy and polarization dependence of multiphoton charge carrier generation rate in diamond," Phys. Rev. E **99**, 104305 (2019).
[17]O. Uteza, B. Bussière, F. Canova, J.-P. Chambaret, P. Delaporte, T. Itina, and M. Sentis, "Laser-induced damage threshold of sapphire in nanosecond picosecond and femtosecond regimes," Appl. Surf. Sci. **254**, 799 (2007).
[18]T. Otobe, Y. Shinohara, S. Sato, and K. Yabana, "Theory for electron excitation in dielectrics under an intense linear and circularly polarized laser fields," J. Phys. Soc. Jpn. **88**, 024706 (2019).
[19]R. Nuter, "Theory of ionization in a crystal with a linear and a circular laser polarization: Influence of the laser wavelength," Phys. Rev. A **108**, 033101 (2023).
[20]L. Sudrie, A. Couairon, M. Franco, B. Lamouroux, B. Prade, S. Tzortzakis, and A. Mysyrowicz, "Femtosecond laser-induced damage and filamentary propagation in fused silica," Phys. Rev. Lett. **89**, 186601 (2002).
[21]H. Reiss and V. Krainov, "Generalized Bessel functions in tunneling ionization," J. Phys. A: Math. Gen. **36**, 5575 (2003).
[22]M. Abramowitz and I. Stegun, *Handbook of Mathematical Functions with Formulas, Graphs, and Mathematical Tables* (National Bureau of Standards, 1972).
[23]K. Hu, Z. Guo, T. cao, S. liu, Z. liu, Z. Li, Q. Xu, K. Chen, and J. Peng, "Study on the polarization dependence of nonlinear absorption of ultrafast laser pulses in bulk fused silica," Opt. Express **30**, 8949 (2022).
[24]*Lasers and Laser-Related Equipment—Test Methods for Laser-Induced Damage Threshold*, ISO 21254-1-212541-4 (2011).
[25]M. Stehlik, F. Wagner, J. Zideluns, F. Lemarchand, J. Lumeau, and L. Gallais, "Beam-size effects on the measurements of sub-picosecond intrinsic laser induced damage threshold of dielectric oxide coatings," Appl. Opt. **60**, 8569 (2021).
[26]L. Gallais, D.-B. Douti, M. Commandré, G. Bataviciuté, E. Pupka, M. Sčiuka, L. Smalakys, and V. Sirutkaitis, "Wavelength dependence of femtosecond laser-induced damage threshold of optical materials," J. Appl. Phys. **117**, 223103 (2015).
[27]A. Ollé, J. Luce, N. Roquin, C. Rouyer, M. Sozet, L. Gallais, and L. Lamiagnère, "Implications of laser beam metrology on laser damage temporal scaling law for dielectric materials in the picosecond regime," Rev. Sci. Instrum. **90**, 073001 (2019).
[28]M. Chambonneau, J.-L. Rullier, P. Grua, and L. Lamaignère, "Wavelength dependence of the mechanisms governing the formation of nanosecond laser-induced damage in fused silica," Opt. Express **26**, 21819 (2018).